Published in final edited form as:
Pflugers Arch. 2013 February ; 465(2): 283–294. doi:10.1007/s00424-012-1178-8.

Ablation of Smooth Muscle Caldesmon Affects the Relaxation Kinetics of Arterial Muscle

Hongqiu Guo, **Renjian Huang**, **Shingo Semba**, **Jolata Kordowska**, **Yang Hoon Huh**, **Yana Khalina-Stackpole**, **Katsuhide Mabuchi**, **Toshio Kitazawa**, and **C.-L. Albert Wang**
Boston Biomedical Research Institute, 64 Grove St., Watertown, MA 02472

Abstract

Smooth muscle caldesmon (h-CaD) is an actin- and myosin-binding protein that reversibly inhibits the actomyosin ATPase activity in vitro. To test the function of h-CaD in vivo, we eliminated its expression in mice. The h-CaD-null animals appeared normal and fertile, although the litter size was smaller. Tissues from the homozygotes lacked h-CaD and exhibited up-regulation of the non-muscle isoform, l-CaD, in visceral, but not vascular tonic smooth muscles. While the Ca^{2+}-sensitivity of force generation of h-CaD-deficient smooth muscle remained largely unchanged, the kinetic behavior during relaxation in arteries was different. Both intact and permeabilized arterial smooth muscle tissues from the knockout animals relaxed more slowly than those of the wild-type. Since this difference occurred after myosin dephosphorylation was complete, the kinetic effect most likely resulted from slower detachment of unphosphorylated cross-bridges. Detailed analyses revealed that the apparently slower relaxation of h-CaD-null smooth muscle was due to an increase in the amplitude of a slower component of the biphasic tension decay. While the identity of this slower process has not been unequivocally determined, we propose it reflects a thin-filament state that elicits fewer re-attached cross-bridges. Our finding that h-CaD modulates the rate of smooth muscle relaxation clearly supports a role in the control of vascular tone.

Keywords

caldesmon; contractile proteins; cross-bridge kinetics; regulation of contraction

Introduction

Myosin phosphorylation, governed by the activities of both myosin light chain kinase (MLCK) and myosin phosphatase [63], is the primary mechanism that regulates smooth muscle contractility, which controls many important physiological processes, including blood pressure, airway resistance, movement of food through the gastro-intestinal system and childbirth. There is, however, evidence that this motor-based on/off switch is not sufficient to account for all aspects of smooth muscle physiology [10,2,68]. Additional regulatory mechanisms may be needed to accommodate complicated situations [67]. One such mechanism involves caldesmon (CaD; [62]) and the thin-filament machinery that is possibly also operating in smooth muscle.

CaD is an actin-binding protein present in both smooth muscle and non-muscle tissues [47,49,70]. The smooth muscle isoform (h-CaD; [8,22]) and the non-muscle isoform (l-CaD; [53,11,64]) are derived from a single gene by alternative splicing [27]. The difference between the two isoforms is an extended single helix of repeating sequences that only exists

Contact Information: C.-L. Albert Wang, 64 Grove Street, Watertown, MA 02472, Telephone: 617-658-7803, Fax: 617-972-1753, wang@bbri.org.

in h-CaD and acts as a "spacer" to separate the more compact N- and the C-terminal domains [43]. It has been shown that the N-terminal end of h-CaD binds to the neck (S2) region of myosin [28,24,72,39], while the C-terminal end of CaD binds actin and inhibits the actomyosin ATPase activity [16,44,56,71]. Based on these and other findings a working model has been put forward for CaD [70], in which h-CaD tethers myosin filaments to actin filaments [72], and together with tropomyosin, sterically blocks actomyosin interactions in the resting state. Upon stimulation, myosin is phosphorylated by MLCK and the C-terminal domain of h-CaD is removed from its inhibitory position on actin either by Ca^{2+}/calmodulin [59,25] or by phosphorylation [51,1], allowing myosin binding and muscle contraction. In this model CaD plays dual roles during smooth muscle contraction. Structurally, it maintains the orderly arrangement of the thick and thin filaments and functionally, it acts as a "molecular brake" to modulate development of contractile force.

The inhibitory action of h-CaD was supported by both biochemical [26] and cellular assays using decoy peptides [29]. Additional evidence came from experiments with removal of h-CaD either by extraction [45] or by antisense- [12] or siRNA- [60] knockdown. In all cases it was observed that after decreasing the level of h-CaD the vascular smooth muscle strip experienced a higher basal tone or smaller active contraction. This is consistent with the hypothesis that smooth muscle regulation includes a thin-filament-based *disinhibition* component. To further test the functional role of h-CaD, we have generated a mouse model in which the h-CaD gene is specifically disrupted by homologous recombination [18]. Although in the h-CaD-null animals there was a compensatory up-regulation of the non-muscle isoform such that drastic phenotypes were not observed, subtle symptoms did exist that could be attributed to the absence of h-CaD. Here we report a novel finding that h-CaD-deficient mouse arterial muscles relaxed more slowly than wild-type (WT) tissues. Our data are consistent with the notion that h-CaD exerts its inhibitory action by facilitating the detachment of ATP-bound, dephosphorylated cross-bridges, rather than preventing phosphorylated cross-bridge formation. Thus, our mouse model not only reveals the physiological function of h-CaD in smooth muscles, but also sheds new light on the mechanism of vascular regulation.

Materials and Methods

Tissue Preparation and Isometric Force Measurements

Adult male C57BL/6 mice (25 ± 4 g) were euthanized by CO_2 according to an IACUC-approved protocol. Aortic and tail arteries and urinary bladder were dissected and freed from fat and soft connective tissues [32]. Arterial vessels and bladder (detrusor) tissues were denuded of endothelial and epithelial layers, respectively. Arterial rings (0.75 mm in length) and bladder smooth muscle strips (0.3 mm in width and 2.5 mm in length) were held by fine hooks of two tungsten needles, one of which was attached to a force transducer (AM801, SensoNor, Horten, Norway). The smooth muscle tissues were then immersed in the normal external solution (see below) in a well on a temperature-controlled Teflon-coated bubble plate [48] to allow rapid solution exchange by sliding the plate to an adjacent well and rapidly freezing with liquid N_2-cooled propane at −150° C. The tissues were repeatedly stimulated with 154 mM K^+ solution at 30 °C until a steady maximal force was attained for each tissue. Myofibrils were prepared from mouse rectum smooth muscle according to published procedures [61] with slight modification (i.e., more extensive homogenization and repeated treatment with 1% Triton).

Permeabilization of Tissues

After several contractions were induced by 154 mM K^+ and by 30 μM α_1-agonist phenylephrine at 30 °C to confirm the integrity of the preparations, the aortic rings were

incubated in relaxing solution for several minutes. For measuring the Ca^{2+}-sensitivity of contractions, the rings were permeabilized with 40 μg/ml purified *Staphylococcus aureus* α-toxin (List, Campbell, CA, USA) at pCa 6.7 buffered with 10 mM EGTA at 30° C and then treated with 10 μM Ca^{2+} ionophore A23187 (Calbiochem) for 20 min at 20° C to deplete the sarcoplasmic reticulum (SR) of Ca^{2+} and to maintain the cytoplasmic Ca^{2+} constant without changes in protein composition [41]. For kinetic studies of arterial contraction and relaxation, the rings were treated with 60 μM β-escin (Sigma) for 30 min at 5°C and then for 15 min at 30° C together with 10 μM A23187, which results in larger pores than with α-toxin and homogenous permeabilization within the tissues [48], thus ensuring faster and more effective control of intracellular Ca^{2+} concentration. All experiments with permeabilized smooth muscle tissues were carried out at 20° C to minimize the deterioration of contractility. To measure the time course of relaxation, we used 10 mM EGTA-containing relaxing solution with 300 μM ML-9 to block MLCK. All solutions were neutralized to pH 7.1 with KOH at 20 °C and an ionic strength of 0.2 M was achieved by using appropriate amounts of potassium methanesulfonate [48].

Solution Compositions

The external solutions for intact smooth muscle rings were prepared as described previously [48]. The normal external solution for intact smooth muscle rings was 150 mM NaCl, 4 mM KCl, 2 mM calcium methanesulphonate, 2 mM magnesium methanesulphonate, 5.6 mM glucose, 30 μM EDTA, and 5 mM *N*-2-hydroxyethylpiperazine-*N*′-2-ethanesulfonic acid (Hepes). To depolarize smooth muscle cells, potassium methanesulphonate (150 mM) was substituted for NaCl of the external solution with all other components used at the same concentration. Both solutions were adjusted to pH 7.4 with Tris.

The standard relaxing solution used for resting states of the α-toxin- and β-escin-permeabilized strips contained the following [48]: 74.1 mM potassium methanesulfonate, 2 mM Mg^{2+}, 4.5 mM MgATP, 1 mM EGTA, 10 mM creatine phosphate, 30 mM piperazine-N,N′-bis(2-ethanesulfonic acid), 1 mM dithiothreitol and pH 7.1 adjusted with KOH at 20°C. In the activating solution, 10 mM EGTA was used and a calculated amount of calcium methanesulfonate was added to give the final desired concentration of free Ca^{2+} ions [32]. Ionic strength of 0.2 M was adjusted with potassium methanesulfonate.

Protein Quantification by Immunoblot Analysis

Protein levels were determined with an Odyssey Infrared Imaging System (LI-COR Biosciences, Lincoln, NE) using dye-conjugated secondary antibodies. Anti-CaD polyclonal antibody (made in house) and anti-β-actin monoclonal antibody (Sigma) were coupled to IRDye™ 700-conjugated anti-rabbit and IRDye™ 800-conjugated anti-mouse antibodies, respectively. h-CaD and l-CaD electrophoretically transferred from SDS polyacrylamide gels to PVDF membranes were readily distinguished on the basis of their molecular weights with the same antibody, thus allowing quantification of both isoforms in the same sample. The band corresponding to anti-β-actin was used as an internal standard for sample loading.

Histology

For histological analysis the aorta were removed immediately after the mice were sacrificed, fixed in phosphate-buffered saline containing 4% formaldehyde, dehydrated with a graded series of ethanol solutions, embedded in paraffin and cut into 3–5 μm sections. Sections were deparaffinized, rehydrated and stained with hematoxylin and eosin. For immunofluorescence imaging, aorta tissues from WT and homozygous knockout (KO) mice were fixed in the phosphate-buffered (PBS) solution containing 4% paraformaldehyde before being embedded in OCT compound and frozen in liquid N_2. After sectioning (7 μm) on a Leica CM3050S cryostat, the samples were stained with Alexa Fluor 532 phalloidin

(200:1 dilution with PBS; for actin) and Hoechst 33258 (1000:1 dilution; for nuclei) according to Eddinger [13]. Elastin was detected by autofluorescence (excited at 488 nm, emission collected at 520 nm). Stained sections were observed using a Leica DMR microscope with 40X objective and epifluorescence illumination.

Electron Microscopy

Immunogold electron microscopy of mouse bladder tissues was carried out [42] with a rabbit polyclonal anti-CaD antibody [41]. All specimens were examined with a Philips 300 electron microscope at 60kV.

Determination of Myosin Light Chain Phosphorylation by Immunoblot Analysis

Rapidly frozen muscle rings were fixed with 10% TCA in acetone at −80 °C overnight, gradually warmed and washed in acetone, dried under vacuum, homogenized in 1% SDS, 15% glycerol, 62.5 mM Tris (pH 6.8), 30 mM DTT, 100 μM Pefabloc (Roche), 10 μM E-64 (Boehringer-Mannheim) and 0.005% bromophenol blue (pH 6.8) then centrifuged. The protein concentration of the supernatant was measured using a protein assay kit (Pierce). Phosphorylation of myosin light chain (MLC) was determined by immunoblot analysis [31] using anti-phospho-MLC antibody (Cell Signaling). The experiments to estimate the total amount of MLC were carried out in duplicate with equal amounts of the same tissue extracts in the same gel and the same nitrocellulose membrane except anti-MLC antibody (Sigma).

Data Analysis and Statistics

All decay traces of isometric tension were analyzed by fitting to a 2-exponential equation by nonlinear regression using KaleidaGraph (Synergy Software, v. 3.6). Results of force measurements, protein level and cell number determinations are all presented as means ± SE. Data were analyzed by Student *t*-test with repeated measurements.

Results

Characterization of h-CaD-null Mice

As described in our preliminary report [18], we have successfully disrupted expression of smooth muscle h-CaD in mice. This was achieved by inserting a tandem stop codon immediately after the exon 3a of the CaD gene beyond the splicing sequence, such that the expression of h-CaD was prematurely terminated, whereas the expression of the shorter isoform, l-CaD, remained intact. The resulting homozygous mice indeed lacked h-CaD, but nevertheless, expressed l-CaD (see below). The percentage of living homozygous offspring from heterozygous parents was only 8.63% (40 out of a total of 472 pups), remarkably lower than the expected value (25%). As noted previously [18], h-CaD-deficient pups were often born with protruding guts, possibly due to failure of ventral wall closure during the late stages of embryogenesis, a birth defect similar to that found in human babies known as omphalocele. Herniated pups could not survive as a result of starvation and/or cannibalism, accounting for part of the missing knockout population. However, the homozygous animals without herniation appeared normal and grew to adulthood without drastic symptoms. While both surviving male and female h-CaD-null mice were fertile, the litter size derived from homozygous crossing was again often smaller (typically $n \leq 3$). In particular, undeveloped and re-absorbed fetuses were found in the pregnant homozygous female, suggesting that deficiency in h-CaD leads to developmental defects other than herniation. The cause and mechanism of this phenotype are not understood at this point and require further investigation.

In the KO mouse l-CaD was found in smooth muscle tissues (Table 1), isolated myofibrils (from mouse rectum; Fig. 1A & B), as well as tissue sections (urinary bladder; Fig. 1C).

Notably, filament arrangement in the KO tissue was inexplicably less well organized compared to WT (Fig. 1C). We did notice that the KO bladder was frequently found to be full even after the animal was sacrificed suggesting that overstretching of the tissue could possibly have resulted in filament disarray. Nevertheless, judging from the close association of the gold particles with myosin filaments in both the KO and WT samples, it appears that the non-muscle isoform occupies the same locations as smooth muscle CaD. The expression of l-CaD indeed increased in response to h-CaD KO except that, as we reported previously [18], this compensatory switchover of CaD isoforms was tissue-dependent. In visceral smooth muscles (such as bladder and intestines) where the content of h-CaD is normally higher [20], the up-regulation of l-CaD in the homozygous tissue was robust, whereas in KO tonic smooth muscles (such as aorta and tail artery), the l-CaD content largely remained unchanged (Table 1). We have estimated the CaD content by quantifying the band intensity of h- or l-CaD on immunoblots normalized to that of β-actin. We found that in WT mice the ratio of h-CaD in bladder to aorta was 5.57 ± 0.76 (n = 3). As for l-CaD, the ratio between bladder and aorta in the WT mice was 1.73 ± 0.24 (n = 4). In KO mice the relative level of l-CaD increased almost 3-fold ($\text{l-CaD}^{KO}/\text{l-CaD}^{WT}$ = 2.91 ± 0.84; n = 4) in bladder smooth muscle, but about the same as that of the WT ($\text{l-CaD}^{KO}/\text{l-CaD}^{WT}$ = 0.98 ± 0.06; n = 5) in aortic smooth muscle (Fig. 2). Similar results were obtained for tail artery, where the relative amount of l-CaD was about the same between the KO and WT tissues ($\text{l-CaD}^{KO}/\text{l-CaD}^{WT}$ = 1.03 ± 0.33; n = 3), although the levels of both h- and l-CaD were 4-fold lower than those in aorta. No gross differences were found in the morphology of KO and WT mouse aorta (Fig. 3A), and immunofluorescence imaging also revealed no substantial differences between the number of cell layers in the media sections of the KO and WT aorta (Fig. 3B). In KO non-muscle tissues, however, there appeared to be a down-regulation of l-CaD (Table 1). The significance of that is unclear at this point.

Physiological Studies of Smooth Muscles from h-CaD-deficient Mice

We have examined the effect of h-CaD on the contractility of aortic smooth muscle by carrying out physiological measurements on tissues isolated from adult WT and homozygous KO mice. Intact mouse aorta developed force upon activation with either membrane depolarization by high concentrations of K^+ or agonist treatment (phenylephrine, ATP and endothelin-1). Among the agonists tested, U46619 (a thromboxane analog; 1–10 μM) induced the largest amount of force in both WT and KO aortas. This maximum force (mean ± SE) per unit cross-section area of h-CaD-null aorta (11.5 ± 1.0 mN/mm^2; n = 7) was about 30% lower than that of the WT (16.5 ± 2.5 mN/mm^2; n = 7), although the *p*-value of this difference exceeds the range of statistical significance ($p = 0.14$) owing to the relatively large animal variation. We did not find significant differences either in the total number of cells in the unit cross-sectional area (33.3 ± 4.4 $/mm^2$ for WT vs. 33.4 ± 4.1 $/mm^2$ for KO; n = 9) or in the total content of actin and myosin (data not shown). On the other hand, the rates of relaxation of the intact aortic tissues from the KO mice were noticeably slower than that from the WT animals (Fig. 4A). For example, the half-time for the force decay after high K^+ (154 mM) stimulation was $t_{1/2}$ = 58.2 ± 12.8 sec for the KO aorta, compared to $t_{1/2}$ = 30.4 ± 1.4 sec for WT ($p = 0.027$). No clear difference was observed for the bladder tissues, which did not have a sustained phase upon stimulation with high K^+ or carbachol (Fig. 4A). Since the contractility of these intact muscle strips might be subject to variations in the intracellular Ca^{2+} concentration ($[Ca^{2+}]_i$), we have measured the forces under permeabilized conditions such that the Ca^{2+} level can be controlled with EGTA-Ca^{2+} buffer externally.

Force was first measured as a function of $[Ca^{2+}]$ in α-toxin-permeabilized aorta, in which endogenous calmodulin was retained [33]. To compare among samples taken from different animals, the measured force was normalized based on the maximum value obtained at pCa

4.5. The force developed in the KO aorta at pCa > 6 was slightly, but consistently ($p < 0.05$) higher than that in the WT aorta. Such a difference, however, disappeared at lower pCa levels, rendering no significant changes in the overall Ca^{2+}-sensitivity between the h-CaD-null and the WT samples (Fig. 4B). We have fitted the data with the Hill equation. The obtained pCa_{50} and Hill coefficients were, respectively, 6.11 ± 0.02 and 1.28 ± 0.18 for the WT (n = 4), and 6.14 ± 0.06 and 1.00 ± 0.04 for KO aorta (n = 4). As a comparison, we have also tested permeabilized urinary bladder smooth muscle strips. The Ca^{2+}-sensitivity, although lower and more cooperative than that found for tonic aortic smooth muscles (of both WT and KO), was nearly identical for the KO and WT bladder samples. The pCa_{50} and Hill coefficients were, respectively, 5.59 ± 0.04 and 2.36 ±0.29 for the WT (n = 8); and 5.53 ± 0.05 and 2.41 ± 0.22 for KO bladder (n = 6). The levels of relative force induced by intermediate Ca^{2+} (pCa 6.3) alone, together with GTPγS (30 μM) or PDBu (1 μM), were all similar in the WT (5 ± 2 %, 64 ± 6 % and 63 ± 3 %, respectively; n = 3) and the KO samples (8 ± 2 %, 62 ± 4 % and 65 ± 3 %, respectively; n = 4; Fig. 4C). In the Ca^{2+}-free solution (10 mM EGTA), the resting tension of either permeabilized tissue was not affected by the presence of staurosporine (1 μM), a non-selective kinase inhibitor. The maximum contraction induced by pCa 4.5 in the presence of GTPγS (30 μM) was also not statistically different ($p = 0.56$) between WT and KO littermates (n = 3).

To further validate the kinetic observations and to achieve better and faster control of Ca^{2+} levels, β-escin was used for tissue permeabilization. Permeabilized aorta rings from WT and KO mouse littermates were first stimulated with the pCa 4.5 solution. After the force reached maximum, the muscles were then relaxed with the Ca^{2+}-free solution (10 mM EGTA with no added Ca^{2+}) in the presence of ML-9 (300 μM) to ensure complete inhibition of MLCK. The relaxation of contractile forces was recorded over a period of 30 min (Fig. 5A). We did not observe significant differences in tension development; however, during relaxation the force invariably showed a slower decay for the KO samples (Fig. 5A; red trace) than for the WT samples (black trace). When analyzed, the time course of the decay could be best fitted with a two-exponential process, the apparent rate constants and the corresponding relative amplitudes (in parentheses) were: $k_1 = 0.46 \pm 0.08\ min^{-1}$ (66 ± 5%) and $k_2 = 0.060 \pm 0.007\ min^{-1}$ (34 ± 5%) for the WT aorta (n = 6), and $k_1 = 0.71 \pm 0.04\ min^{-1}$ (32 ± 3%) and $k_2 = 0.081 \pm 0.008\ min^{-1}$ (68 ± 3%) for the KO sample (n = 6; Table 2). To facilitate the fitting the initial points near the short plateau right after changing to relaxing solution were truncated. According to Khromov et al. [30], this “lag phase” may reflect MLC dephosphorylation. We did not find any difference in this phase between WT and KO aorta (Fig. 5A). Based on our analysis, there existed two first-order kinetic processes during aortic relaxation, one being 8- to 9-fold faster than the other. Despite the appearance of slower relaxation for the KO samples, the rate constants of both components were actually higher for KO than WT tissues ($p < 0.05$). What made the overall slowness of the KO was the relative amplitude of the two components. Thus, the apparently slower relaxation observed for the KO samples was due to a greater contribution of the slower component of the relaxation process for the h-CaD-null muscle strips, rather than a decrease of the rate constants.

We also performed the same experiments on tail arteries. The results were qualitatively similar to those of aorta, i.e., the h-CaD-deficient tissues relaxed more slowly than the WT samples, except that there was a more extensive lag phase. The lag phase appeared longer for the KO sample (35 ± 6 sec, n = 6) than the WT sample (24 ± 2 sec, n = 6, $p = 0.04$; Fig. 5B). Whether this indicates a difference in the rate of MLC dephosphorylation remains to be seen. For the kinetic parameters of tail arteries, the apparent rate constants and the corresponding relative amplitudes were: $k_1 = 1.71 \pm 0.15\ min^{-1}$ (81 ± 5%) and $k_2 = 0.40 \pm 0.09\ min^{-1}$ (19 ± 5%) for the WT aorta (n = 6), and $k_1 = 1.55 \pm 0.26\ min^{-1}$ (62 ± 2%) and $k_2 = 0.34 \pm 0.07\ min^{-1}$ (38 ± 2%) for the KO sample (n = 6; Table 2). Note that although the

rate constants of both fast and slow components were comparable ($p > 0.5$) between WT and KO tail arteries, which relaxed 2 to 3 times faster than the aorta, the major change was still the relative amplitudes of the two components. The characteristics of relaxation kinetics did not seem to be related to the amount of CaD in the tissue, because urinary bladder smooth muscle, which had a higher level of h- and l-CaD than aorta in both WT and KO tissues (see above; Table 1), also relaxed at a faster rate than aorta (not shown).

Myosin Light Chain Phosphorylation during Relaxation

Since MLCK activity was abolished during relaxation with the removal of Ca^{2+} and inclusion of EGTA and ML-9, we tested whether the slower relaxation rate exhibited by the h-CaD-null aortic muscles was due to an altered myosin phosphatase activity. The level of MLC phosphorylation of the muscle strips was determined by Western blot analysis as a function of time. Four time points were taken: at t = 0 (immediately after exposure to relaxation buffer), 2, 5, and 10 min after the initiation of relaxation (Fig. 6). The results with both anti-MLC and anti-phospho-MLC antibodies showed that while similar levels of MLC phosphorylation were attained for both WT and KO samples at t = 0, there was essentially no detectable phosphorylated MLC in either sample after 2 min exposure to the relaxing solution (Fig. 6). These results are consistent with earlier reports that MLC dephosphorylation is faster than contractile force decay [34,30,40]. A similar time course of MLC dephosphorylation was observed for rabbit artery under similar conditions [32,48,35]. On the other hand, the major mechanical difference between WT and KO aorta was only seen after 5 min (Fig. 5). Since at this time point the fast component of force decay was already nearly finished and so was dephosphorylation of MLC, it appeared that it was mainly the slower component of the decay process, which may or may not have any bearing on MLC dephosphorylation, that contributed to the differences between the KO and WT tissues.

Discussion

The functional role of h-CaD in smooth muscle regulation has been studied for more than three decades. The general consensus is that h-CaD inhibits actomyosin interaction by binding to actin and blocking the myosin-binding site; the inhibition is reversed by either Ca^{2+}/CaM or by Erk-mediated phosphorylation. This view is supported by many experimental observations, albeit indirectly, including contraction induced by competing peptides [29], augmented basal contraction [12] or heightened Ca^{2+}-sensitivity [45] by removal of h-CaD, and enhanced relaxation by exogenously added CaD [3]. CaD was also proposed to function as a “latch” for sustained tension maintenance without ATP hydrolysis [46].

The smooth muscle-specific isoform of CaD, h-CaD, is present in all vertebrate smooth muscle tissues. Although there has been a controversy on whether or not the h-CaD content varies among different types of smooth muscles [21,19,36,37], we did observe a lower h-CaD level in murine vascular smooth muscles (aorta and tail artery) than in visceral smooth muscles (urinary bladder; Table 1). Since h-CaD is thought to play an inhibitory role during muscle contraction, the higher expression level of h-CaD in visceral smooth muscles might contribute to the rapidness of the transient contraction (hence “phasic”). However, when the expression of h-CaD was abolished, l-CaD became up-regulated only in visceral smooth muscles [18]. While this may suggest that CaD (of either isoform) is indispensable in these muscles, it also implies that l-CaD can at least partially substitute for h-CaD. On the other hand, vascular smooth muscles, which contain less h-CaD in the WT animals, did not show a clear isoform switchover in the KO mice. Thus, such KO muscles have a net decrease in the total content of CaD, providing an opportunity to reveal the physiological function of h-CaD.

A more interesting finding was the effect of h-CaD abrogation on the kinetics of arterial contractility: Total withdrawal of h-CaD caused an apparently slower rate of relaxation. Either intact or permeabilized aortic strips from both WT and KO animals developed forces at a similar rate, but the KO tissues relaxed more slowly than the WT tissues (Figs. 4A and 5A). Measurements of MLC phosphorylation indicated that the observed difference is not directly due to a slower dephosphorylation rate of myosin in the h-CaD-null tissue (Fig. 6). An indirect effect, however, cannot be ruled out at this point, although it may still be unlikely given that KO tail arteries exhibited a longer lag phase (and presumably, slower MLC dephosphorylation) than WT tissues, but did not show greater differences in relaxation kinetics. A more likely explanation is that h-CaD affects the cycling rate of cross-bridges formed by myosin that is completely or nearly completely dephosphorylated. It has been shown previously that the rate of relaxation of skinned smooth muscle is accelerated when CaD, but not calponin, is loaded exogenously [3]. Our observation seems to be in line with that report, although the mechanism of such an effect remains elusive.

When the time course of the contractile force relaxation was analyzed, it became clear that for both WT and KO tissues there were two components in the decay kinetics following the “plateau phase” or lag phase [30]. The values of the two rate constants varied with tissue types; tail artery relaxed 3 to 5 times faster than aorta (Table 2). However, the apparent longer decay time for the h-CaD-deficient tissue was not due to a slower rate constant, but rather, to an increased contribution of the slower component of the decay process. Bi-exponential force decay during relaxation of skinned smooth muscle tissues has been observed previously [3], but the identity of each component was not explicitly discussed. The question of interest is what reactions these two components correspond to.

The observed difference in the relaxation kinetics could be due to different protein isoforms, although we do not know whether this is the case, or if it is, the identity of the altered protein. However, we think it is unlikely to be smooth muscle myosin heavy chain, whose two isoforms, SM-A (tonic) and SM-B (phasic), exhibit different steady-state ATPase activities [4], because in mouse aorta myosin is nearly 100% in the form of SM-A [5], yet the force decays bi-exponentially (Table 2). The kinetic effect could have also stemmed from changes in the cross-bridge population across various states in the cycle at the onset of relaxation, or alternatively, from changes in the cross-bridge cycling itself. Upon relaxation, phosphorylation of MLC ceases to continue, and the cross-bridge becomes completely dephosphorylated. Since the release of product (i.e., ADP) is slow [52], the most populated state after dephosphorylation is A•M•D, where A, M and D represent, respectively, actin, myosin and ADP. A•M•D continues to cycle, according to the model of Somlyo and coworkers [15], which allows for the dephosphorylated cross-bridges to re-attach cooperatively, until all the cross-bridge are eventually detached.

Our data indicate that there exist two cycling paths for the dephosphorylated cross-bridge (i.e., latchbridge), each being rate-limited by a reaction step, one faster than the other. In normal smooth muscles where h-CaD is present, the majority of the cross-bridges (66% for aorta and 81% for tail artery; Table 2) cycles along a path that is rate-limited by the fast component. When h-CaD is not present, a fraction of the cross-bridge is diverted to the path that is rate-limited by the slow component, such that the amplitude of this slower component increases (from 34% to 68% for aorta and from 19% to 38% in tail artery). It should be noted that here we assumed that the rate is an intrinsic property for a given biological process, while the amplitude is more easily altered by perturbations such as eliminating a protein species. The fact that both fast and slow components existed in the force decay of the WT sample, and that the difference between the WT and the KO samples was greater for the amplitude than for the rate constants of the two components, seemed to support our assumption.

In search of a mechanistic explanation for the observed relaxation kinetics, one could draw some lessons from work done on the striated muscle system. According to Stehle et al.[65], muscle relaxation involves two mutually coupled events: (1) cross-bridge detachment and (2) change of the thin filament from an active to inactive state. There is plenty of evidence that in striated muscle the latter event, which is in rapid equilibrium [7], occurs before the onset of the former [9]. Since inactivation of thin filaments does not change the sarcomere length [66], this event is thought to correspond to the initial slow or lag phase before the rapid force decay, which is caused by cross-bridge detachment. In the case of smooth muscle, the lag phase is ascribed to MLC dephosphorylation [30], but it may also include change in the state of the thin filament. According to the steric-blocking model [6,69], this would be movement of troponin-tropomyosin, or for smooth muscle, CaD-tropomyosin, back to a position on the actin filament that hinders myosin binding. It is conceivable that this “off-position” might be under strain, because the dephosphorylated cross-bridges are still attached. Assuming that there are two possible positions (e.g., positions similar to the B- and the C-states; [50]) for CaD-tropomyosin to occupy, one having more extensive overlap with the binding site for myosin than the other, the cross-bridge would exhibit different abilities to re-attach, resulting in different net detachment rates of cross-bridges and hence the observed biphasic decay. Our data then suggest that when h-CaD is absent, fewer tropomyosin molecules are at or near the blocking position. In other words, the return of smooth muscle tropomyosin to the proper inhibitory position upon relaxation needs help from h-CaD. Indeed, it has been demonstrated that in striated muscle the movement of tropomyosin is facilitated by troponin subunits [17,38]. CaD may very well play a troponin-like role in smooth muscle both structurally and functionally.

On the basis of its ability to simultaneously interact with both actin and myosin in vitro and thus to tether thick and thin filaments [23,28], h-CaD has previously been suggested to help maintain the latchbridge in vivo [46]. This idea, although attractive, cannot explain why in visceral smooth muscles where the h-CaD content is high, no strong latch phenomenon has been observed. Furthermore, if h-CaD were to contribute to latchbridge maintenance, one would expect a faster detachment rate of cross-bridges in the h-CaD-null tissue, which might be the case for aorta, but was not observed for tail artery (Table 2). Our results suggest that, rather than *maintaining* the latchbridge, h-CaD actually *facilitates* the detachment of the latchbridge in the presence of ATP, thus promoting faster relaxation. Such an effect is consistent with the generally observed inhibitory properties of CaD. That h-CaD promotes latchbridge dissociation has previously escaped detection, probably because the second phase is always only a minor component as long as h-CaD is present in smooth muscle tissues. It should be pointed out that the inhibitory action of h-CaD on cross-bridge attachment could still occur. That inhibition is due to actin binding of the C-terminal region of the molecule, while the action regarding the latchbridge does not need to be associated with the same region of h-CaD. Interestingly, a similar kinetic behavior was observed in another mouse model where the myosin-binding site of CaD was deleted [57]. Whether the CaD-myosin interaction is related to the phenotype is an intriguing question awaiting further investigation.

It is known that while at the resting state the MLC phosphorylation level is not zero (10–20% of total MLC) and no active force can be detected [55]. One potential explanation is that any basal contractility could be inhibited by h-CaD. If this were the case, one would expect a higher resting tone and a higher Ca-sensitivity for force development in the h-CaD-null tissue. The lack of a clear leftward shift in the force-pCa plot from our experiments seems to argue against this possibility. There was, however, a small but significant increase in contraction in the KO aorta when $6 < pCa < 7$, which disappeared at both higher and lower pCa values (asterisks, Fig. 4B). It is possible that in aorta any effect of CaD at high Ca^{2+} concentrations could be neutralized by Ca^{2+}/calmodulin, resulting in no net difference

in contractility between the WT and the KO, whereas at relatively low [Ca^{2+}] the active force induced by resting phosphorylated cross-bridges is suppressed by l-CaD present in the KO tissues. In bladder the difference between KO and WT was even less, and the Ca^{2+} dependence of active force was steeper than that of aorta. This is in contrast to previous studies where an increase in force at low Ca^{2+} was observed when h-CaD was extracted from skinned taenia coli, and the change was partially reversed by reconstitution of CaD [45,54]. We believe that, although for visceral smooth muscle there might indeed be a more robust CaD effect than in vascular smooth muscle, such an effect was masked by the up-regulation of l-CaD in the KO tissues, rendering a decreased net difference in our experiments. In an earlier study where the h-CaD content in the intact swine carotid smooth muscle was decreased by 60% with anti-sense oligonucleotides, there was a correspondent decrease of 62% in contractility that was interpreted as a raised basal tone [12]. Although we have not observed a higher basal force, we did find that forces generated by h-CaD-deficient tissues tend to be lower than the WT. Whether this is related to the change in filamentous organization as seen in bladder (Fig. 1C) requires further study. To test the true effect on the basal tone, one also needs to perform rescue experiments or to generate mice in which both CaD isoforms are knocked out.

The action of h-CaD may thus be two-fold: During the resting state or when the level of MLC phosphorylation is low, CaD inhibits the actomyosin interaction via its C-terminal region. Upon activation, this region of CaD is removed from its inhibitory position, either by Ca^{2+}/calmodulin, or MAPK-mediated phosphorylation [14], or by direct competition with myosin [58]. This function is the “conventional” role of h-CaD that has been well described. A more novel action of h-CaD turns up when relaxation commences and MLC is dephosphorylated. Under this circumstance CaD helps tropomyosin to move from the on-position to the off-position, permitting more effective net detachment of cross-bridges upon relaxation. In this sense CaD might indeed works like a molecular brake, except that such a function is visible only when MLC is not phosphorylated, enabling the muscle to relax more promptly. When h-CaD is absent, vascular smooth muscle relaxes more slowly. This may conceivably elevate the tone. Our study thus raises the possibility that h-CaD is involved in the regulation of vascular tone.

Acknowledgments

This work was supported by grants from NIH (P01-AM41637 and R01-HL92252). The authors wish to thank Dr. Hiroshi Mashimo for his assistance in the early phase of this project, and Dr. Lynne Coluccio for reading the manuscript.

References

1. Adam LP, Haeberle JR, Hathaway DR. Phosphorylation of caldesmon in arterial smooth muscle. J Biol Chem. 1989; 264 (13):7698–7703. [PubMed: 2708386]
2. Aksoy MO, Murphy RA, Kamm KE. Role of Ca2+ and myosin light chain phosphorylation in regulation of smooth muscle. Am J Physiol. 1982; 242:C109–116. [PubMed: 6895816]
3. Albrecht K, Schneider A, Liebetrau C, Ruegg JC, Pfitzer G. Exogenous caldesmon promotes relaxation of guinea-pig skinned taenia coli smooth muscles: inhibition of cooperative reattachment of latch bridges? Pflugers Arch. 1997; 434 (5):534–542. [PubMed: 9242716]
4. Babu GJ, Loukianov E, Loukianova T, Pyne GJ, Huke S, Osol G, Low RB, Paul RJ, Periasamy M. Loss of SM-B myosin affects muscle shortening velocity and maximal force development. Nat Cell Biol. 2001; 3 (11):1025–1029. [PubMed: 11715025]
5. Babu GJ, Pyne GJ, Zhou Y, Okwuchukuasanya C, Brayden JE, Osol G, Paul RJ, Low RB, Periasamy M. Isoform switching from SM-B to SM-A myosin results in decreased contractility and altered expression of thin-filament/regulatory proteins. Am J Physiol Cell Physiol. 2004; 287 (3):C723–729. [PubMed: 15140746]

6. Bremel RD, Weber A. Cooperation within actin filament in vertebrate skeletal muscle. Nat New Biol. 1972; 238 (82):97–101. [PubMed: 4261616]
7. Brenner B, Chalovich JM. Kinetics of thin filament activation probed by fluorescence of N-((2-(iodoacetoxy)ethyl)-N-methyl)amino-7-nitrobenz-2-oxa-1,3-diazole-labeled troponin I incorporated into skinned fibers of rabbit psoas muscle: implications for regulation of muscle contraction. Biophys J. 1999; 77 (5):2692–2708. [PubMed: 10545369]
8. Bryan J, Imai M, Lee R, Moore P, Cook RG, Lin WG. Cloning and expression of a smooth muscle caldesmon. J Biol Chem. 1989; 264 (23):13873–13879. [PubMed: 2760048]
9. de Tombe PP, Belus A, Piroddi N, Scellini B, Walker JS, Martin AF, Tesi C, Poggesi C. Myofilament calcium sensitivity does not affect cross-bridge activation-relaxation kinetics. Am J Physiol Regul Integr Comp Physiol. 2007; 292 (3):R1129–1136. [PubMed: 17082350]
10. Dillon PF, Aksoy MO, Driska SP, Murphy RA. Myosin phosphorylation and the cross-bridge cycle in arterial smooth muscle. Science. 1981; 211:495–497. [PubMed: 6893872]
11. Dingus J, Hwo S, Bryan J. Identification by monoclonal antibodies and characterization of human platelet caldesmon. J Cell Biol. 1986; 102 (5):1748–1757. [PubMed: 3517005]
12. Earley JJ, Su X, Moreland RS. Caldesmon inhibits active crossbridges in unstimulated vascular smooth muscle: an antisense oligodeoxynucleotide approach. Circ Res. 1998; 83 (6):661–667. [PubMed: 9742062]
13. Eddinger TJ, Schiebout JD, Swartz DR. Smooth muscle adherens junctions associated proteins are stable at the cell periphery during relaxation and activation. Am J Physiol Cell Physiol. 2005; 289 (6):C1379–1387. [PubMed: 16033907]
14. Foster DB, Huang R, Hatch V, Craig R, Graceffa P, Lehman W, Wang C-LA. Modes of caldesmon binding to actin: sites of caldesmon contact and modulation of interactions by phosphorylation. J Biol Chem. 2004; 279 (51):53387–53394. [PubMed: 15456752]
15. Fuglsang A, Khromov A, Torok K, Somlyo AV, Somlyo AP. Flash photolysis studies of relaxation and cross-bridge detachment: higher sensitivity of tonic than phasic smooth muscle to MgADP. J Muscle Res Cell Motil. 1993; 14 (6):666–677. [PubMed: 8126226]
16. Fujii T, Imai M, Rosenfeld GC, Bryan J. Domain mapping of chicken gizzard caldesmon. J Biol Chem. 1987; 262 (6):2757–2763. [PubMed: 2434491]
17. Galinska-Rakoczy A, Engel P, Xu C, Jung H, Craig R, Tobacman LS, Lehman W. Structural basis for the regulation of muscle contraction by troponin and tropomyosin. J Mol Biol. 2008; 379 (5): 929–935. [PubMed: 18514658]
18. Guo H, Wang C-LA. Specific disruption of smooth muscle caldesmon expression in mice. Biochem Biophys Res Commun. 2005; 330 (4):1132–1137. [PubMed: 15823561]
19. Haeberle JR, Hathaway DR. Correspondence. J Muscle Res Cell Motility. 1992; 13:584–585.
20. Haeberle JR, Hathaway DR, Smith CL. Caldesmon content of mammalian smooth muscles. J Muscle Res Cell Motil. 1992; 13 (1):81–89. [PubMed: 1556173]
21. Haeberle JR, Hathaway DR, Smith CL. Caldesmon content of mammalian smooth muscles [see comments]. J Muscle Res Cell Motil. 1992; 13 (1):81–89. [PubMed: 1556173]
22. Hayashi K, Kanda K, Kimizuka F, Kato I, Sobue K. Primary structure and functional expression of h-caldesmon complementary DNA. Biochem Biophys Res Commun. 1989; 164 (1):503–511. [PubMed: 2803315]
23. Hemric ME, Chalovich JM. Effect of caldesmon on the ATPase activity and the binding of smooth and skeletal myosin subfragments to actin. J Biol Chem. 1988; 263 (4):1878–1885. [PubMed: 2962997]
24. Hemric ME, Chalovich JM. Characterization of caldesmon binding to myosin. J Biol Chem. 1990; 265 (32):19672–19678. [PubMed: 2246251]
25. Horiuchi KY, Miyata H, Chacko S. Modulation of smooth muscle actomyosin ATPase by thin filament associated proteins. Biochem Biophys Res Commun. 1986; 136 (3):962–968. [PubMed: 2941015]
26. Huang R, Wang CL. A caldesmon peptide activates smooth muscle via a mechanism similar to ERK-mediated phosphorylation. FEBS Lett. 2006; 580 (1):63–66. [PubMed: 16343491]
27. Humphrey MB, Herrera-Sosa H, Gonzalez G, Lee R, Bryan J. Cloning of cDNAs encoding human caldesmons. Gene. 1992; 112 (2):197–204. [PubMed: 1555769]

28. Ikebe M, Reardon S. Binding of caldesmon to smooth muscle myosin. J Biol Chem. 1988; 263 (7): 3055–3058. [PubMed: 3257755]
29. Katsuyama H, Wang C-LA, Morgan KG. Regulation of vascular smooth muscle tone by caldesmon. J Biol Chem. 1992; 267 (21):14555–14558. [PubMed: 1386078]
30. Khromov A, Somlyo AV, Trentham DR, Zimmermann B, Somlyo AP. The role of MgADP in force maintenance by dephosphorylated cross-bridges in smooth muscle: a flash photolysis study. Biophys J. 1995; 69 (6):2611–2622. [PubMed: 8599668]
31. Kitazawa T, Eto M, Woodsome TP, Brautigan DL. Agonists trigger G protein-mediated activation of the CPI-17 inhibitor phosphoprotein of myosin light chain phosphatase to enhance vascular smooth muscle contractility. Journal of Biological Chemistry. 2000; 275 (14):9897–9900. [PubMed: 10744661]
32. Kitazawa T, Gaylinn BD, Denney GH, Somlyo AP. G-protein-mediated Ca2+-sensitization of smooth muscle contraction through myosin light chain phosphorylation. J Biol Chem. 1991; 266:1708–1715. [PubMed: 1671041]
33. Kitazawa T, Kobayashi S, Horiuti K, Somlyo AV, Somlyo AP. Receptor-coupled, permeabilized smooth muscle : Role of the phosphatidylinositol cascade, G-proteins, and modulation of the contractile response to Ca^{2+} J Biol Chem. 1989; 264:5339–5342. [PubMed: 2494163]
34. Kuhn H, Tewes A, Gagelmann M, Guth K, Arner A, Ruegg JC. Temporal relationship between force, ATPase activity, and myosin phosphorylation during a contraction/relaxation cycle in a skinned smooth muscle. Pflugers Arch. 1990; 416 (5):512–518. [PubMed: 2146588]
35. Lee MR, Li L, Kitazawa T. Cyclic GMP causes Ca2+ desensitization in vascular smooth muscle by activating the myosin light chain phosphatase. J Biol Chem. 1997; 272 (8):5063–5068. [PubMed: 9030570]
36. Lehman W, Denault D, Marston S. Novel immunological technique. J Muscle Res Cell Motil. 1992; 13 (5):582–585. [PubMed: 1460085]
37. Lehman W, Denault D, Marston S. The caldesmon content of vertebrate smooth muscle. Biochim Biophys Acta. 1993; 1203 (1):53–59. [PubMed: 8218392]
38. Lehman W, Galinska-Rakoczy A, Hatch V, Tobacman LS, Craig R. Structural basis for the activation of muscle contraction by troponin and tropomyosin. J Mol Biol. 2009; 388 (4):673–681. [PubMed: 19341744]
39. Li Y, Zhuang S, Guo H, Mabuchi K, Lu RC, Wang C-LA. The major myosin-binding site of caldesmon resides near its N-terminal extreme. J Biol Chem. 2000; 275 (15):10989–10994. [PubMed: 10753900]
40. Lubomirov LT, Reimann K, Metzler D, Hasse V, Stehle R, Ito M, Hartshorne DJ, Gagov H, Pfitzer G, Schubert R. Urocortin-induced decrease in Ca2+ sensitivity of contraction in mouse tail arteries is attributable to cAMP-dependent dephosphorylation of MYPT1 and activation of myosin light chain phosphatase. Circ Res. 2006; 98 (9):1159–1167. [PubMed: 16574904]
41. Mabuchi K, Li Y, Carlos A, Wang CL, Graceffa P. Caldesmon exhibits a clustered distribution along individual chicken gizzard native thin filaments. J Muscle Res Cell Motil. 2001; 22 (1):77–90. [PubMed: 11563552]
42. Mabuchi K, Li Y, Tao T, Wang C-LA. Immunocytochemical localization of caldesmon and calponin in chicken gizzard smooth muscle. J Muscle Res Cell Motil. 1996; 17 (2):243–260. [PubMed: 8793726]
43. Mabuchi K, Wang C-LA. Electron microscopic studies of chicken gizzard caldesmon and its complex with calmodulin. J Muscle Res Cell Motil. 1991; 12 (2):145–151. [PubMed: 2061408]
44. Makuch R, Walsh MP, Dabrowska R. Location of the calmodulin- and actin-binding domains at the C-terminus of caldesmon. FEBS Lett. 1989; 247 (2):411–414. [PubMed: 2523821]
45. Malmqvist U, Arner A, Makuch R, Dabrowska R. The effects of caldesmon extraction on mechanical properties of skinned smooth muscle fibre preparations. Pflugers Arch. 1996; 432 (2): 241–247. [PubMed: 8662300]
46. Marston SB. What is latch? New ideas about tonic contraction in smooth muscle. J Muscle Res Cell Motil. 1989; 10 (2):97–100. [PubMed: 2668329]
47. Marston, SB.; Huber, PAJ. Caldesmon. In: Bárány, M., editor. Biochemistry of Smooth Muscle Contraction. Academic Press, Inc; San Diego, CA: 1996. p. 77-90.

48. Masuo M, Reardon S, Ikebe M, Kitazawa T. A novel mechanism for the Ca2+-sensitizing effect of protein kinase C on vascular smooth muscle: Inhibition of myosin light chain phosphatase. J Gen Physiol. 1994; 104 (2):265–286. [PubMed: 7807049]
49. Matsumura F, Yamashiro S. Caldesmon. Curr Opin Cell Biol. 1993; 5 (1):70–76. [PubMed: 8448032]
50. McKillop DF, Geeves MA. Regulation of the interaction between actin and myosin subfragment 1: evidence for three states of the thin filament. Biophys J. 1993; 65 (2):693–701. [PubMed: 8218897]
51. Ngai PK, Walsh MP. The effects of phosphorylation of smooth-muscle caldesmon. Biochem J. 1987; 244 (2):417–425. [PubMed: 2822003]
52. Nishiye E, Somlyo AV, Torok K, Somlyo AP. The effects of MgADP on cross-bridge kinetics: a laser flash photolysis study of guinea-pig smooth muscle. J Physiol. 1993; 460:247–271. [PubMed: 8487195]
53. Owada MK, Hakura A, Iida K, Yahara I, Sobue K, Kakiuchi S. Occurrence of caldesmon (a calmodulin-binding protein) in cultured cells: comparison of normal and transformed cells. Proc Natl Acad Sci U S A. 1984; 81 (10):3133–3137. [PubMed: 6328499]
54. Pfitzer G, Schroeter M, Hasse V, Ma J, Rosgen KH, Rosgen S, Smyth N. Is myosin phosphorylation sufficient to regulate smooth muscle contraction? Adv Exp Med Biol. 2005; 565:319–328. discussion 328 405–315. [PubMed: 16106985]
55. Rembold CM, Wardle RL, Wingard CJ, Batts TW, Etter EF, Murphy RA. Cooperative attachment of cross bridges predicts regulation of smooth muscle force by myosin phosphorylation. Am J Physiol Cell Physiol. 2004; 287 (3):C594–602. [PubMed: 15151901]
56. Riseman VM, Lynch WP, Nefsky B, Bretscher A. The calmodulin and F-actin binding sites of smooth muscle caldesmon lie in the carboxyl-terminal domain whereas the molecular weight heterogeneity lies in the middle of the molecule. J Biol Chem. 1989; 264 (5):2869–2875. [PubMed: 2914935]
57. Schroeter MM, Hasse V, Roesgen S, Roesgen K-H, Smyth NR, Diepold A, Chalovich JM, Pfitzer G. Probing the myosin binding region of caldesmon in a knock-out mouse model. Biophys J. 2005; 88:359a.
58. Sen A, Chen YD, Yan B, Chalovich JM. Caldesmon reduces the apparent rate of binding of myosin S1 to actin- tropomyosin. Biochemistry. 2001; 40 (19):5757–5764. [PubMed: 11341841]
59. Smith CW, Marston SB. Disassembly and reconstitution of the Ca2+-sensitive thin filaments of vascular smooth muscle. FEBS Lett. 1985; 184 (1):115–119. [PubMed: 3987897]
60. Smolock EM, Trappanese DM, Chang S, Wang T, Titchenell P, Moreland RS. siRNA-mediated knockdown of h-caldesmon in vascular smooth muscle. Am J Physiol Heart Circ Physiol. 2009; 297 (5):H1930–1939. [PubMed: 19767533]
61. Sobieszek A, Bremel RD. Preparation and properties of vertebrate smooth-muscle myofibrils and actomyosin. Eur J Biochem. 1975; 55 (1):49–60. [PubMed: 126155]
62. Sobue K, Muramoto Y, Fujita M, Kakiuchi S. Purification of a calmodulin-binding protein from chicken gizzard that interacts with F-actin. Proc Natl Acad Sci U S A. 1981; 78 (9):5652–5655. [PubMed: 6946503]
63. Somlyo AP, Somlyo AV. Signal transduction and regulation in smooth muscle. Nature. 1994; 372 (6503):231–236. [PubMed: 7969467]
64. Stafford WF, Jancso A, Graceffa P. Caldesmon from rabbit liver: molecular weight and length by analytical ultracentrifugation. Arch Biochem Biophys. 1990; 281 (1):66–69. [PubMed: 2383024]
65. Stehle R, Iorga B, Pfitzer G. Calcium regulation of troponin and its role in the dynamics of contraction and relaxation. Am J Physiol Regul Integr Comp Physiol. 2007; 292 (3):R1125–1128. [PubMed: 17158261]
66. Stehle R, Kruger M, Pfitzer G. Force kinetics and individual sarcomere dynamics in cardiac myofibrils after rapid ca(2+) changes. Biophys J. 2002; 83 (4):2152–216. [PubMed: 12324432]
67. Stull JT, Gallagher PJ, Herring BP, Kamm KE. Vascular smooth muscle contractile elements. Cellular regulation. Hypertension. 1991; 17 (6 Pt 1):723–732. [PubMed: 2045132]

68. Tansey MG, Hori M, Karaki H, Kamm KE, Stull JT. Okadaic acid uncouples myosin light chain phosphorylation and tension in smooth muscle. FEBS Lett. 1990; 270:219–221. [PubMed: 2171992]

69. Vibert P, Craig R, Lehman W. Steric-model for activation of muscle thin filaments. J Mol Biol. 1997; 266 (1):8–14. [PubMed: 9054965]

70. Wang C-LA. Caldesmon and smooth-muscle regulation. Cell Biochem Biophys. 2001; 35 (3):275–288. [PubMed: 11894847]

71. Wang C-LA, Wang L-WC, Xu SA, Lu RC, Saavedra-Alanis V, Bryan J. Localization of the calmodulin- and the actin-binding sites of caldesmon. J Biol Chem. 1991; 266 (14):9166–9172. [PubMed: 2026616]

72. Wang Z, Jiang H, Yang ZQ, Chacko S. Both N-terminal myosin-binding and C-terminal actin-binding sites on smooth muscle caldesmon are required for caldesmon-mediated inhibition of actin filament velocity. Proc Natl Acad Sci U S A. 1997; 94 (22):11899–11904. [PubMed: 9342334]

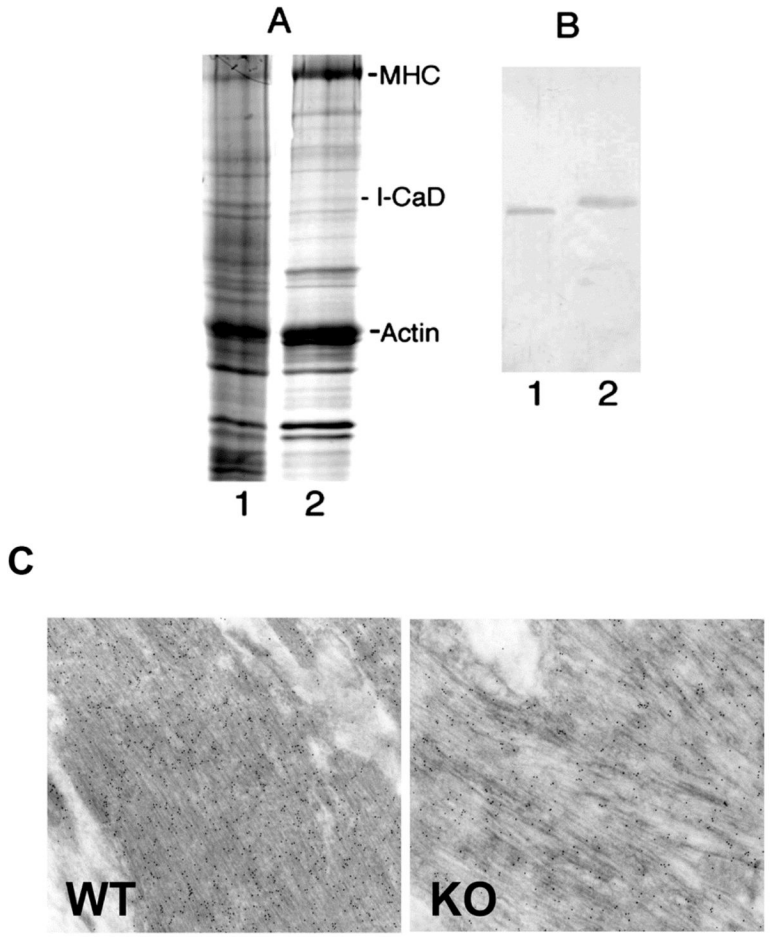

Fig. 1.

l-CaD is present in h-CaD-null smooth muscle tissues. (**A**) Coomassie staining of total extract (Lane 1) and the myofibril fraction (Lane 2) of homozygous mouse rectum. (**B**) Immunoblot of l-CaD from chicken liver (Lane 1) and the rectum myofibril fraction (Lane 2) from KO mouse as in (A). (**C**) Immunogold electron micrographic images show that the distribution of l-CaD in the smooth muscle tissue from the urinary bladder of the KO mouse resembles that of h-CaD in the WT sample. The somewhat less organized filament arrangement in the KO sample might reflect the muscle having been more stretched than the WT tissue, although both samples were treated in the same way. However, note that the gold particles in the KO tissue are closely associated with filamentous structures in a similar fashion as in the WT tissue. Magnification: 15960X.

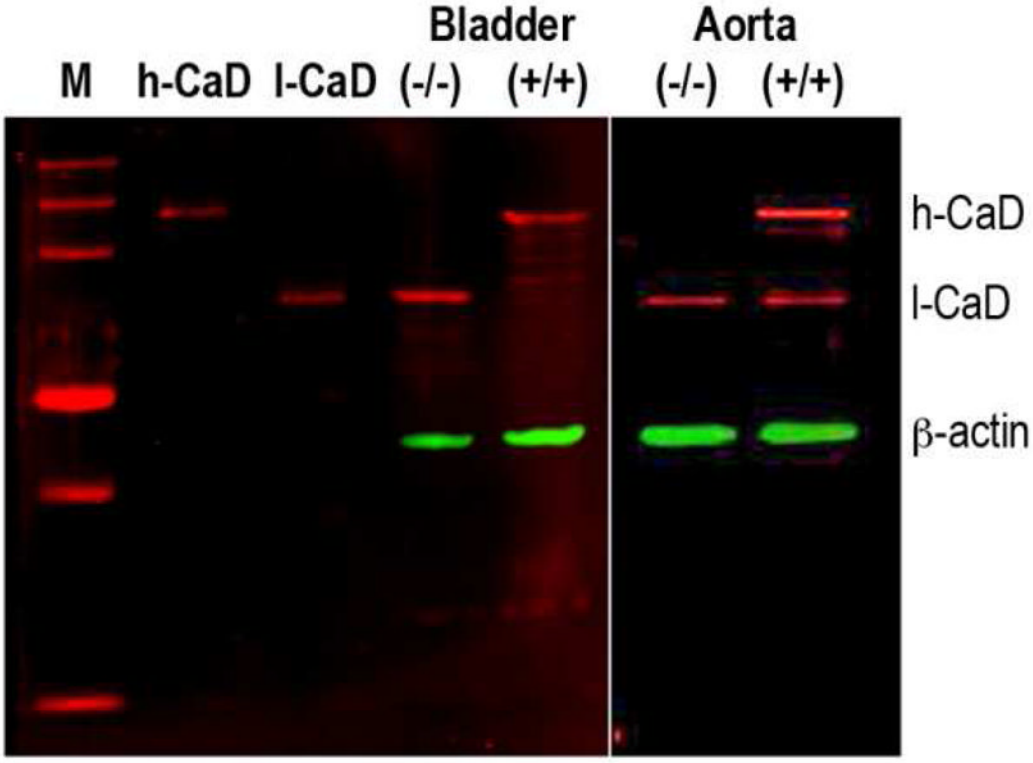

Fig. 2.

Immunoblot analysis by Odyssey imaging of tissue extracts from bladder and aorta of WT and KO mice. WT aorta has less h-CaD than does WT bladder, and the up-regulation of l-CaD in the KO animal is less robust. β-actin was used as an internal reference.

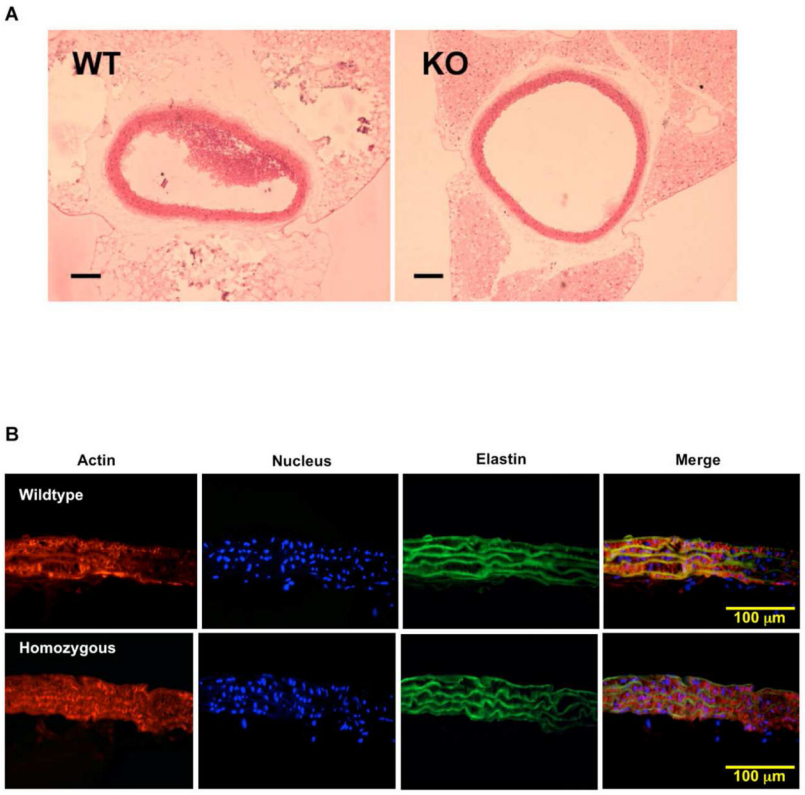

Fig. 3.

Hematoxylin and eosin stained transverse histological sections (**A**) and immunofluorescence imaging of transverse cryostat sections (**B**) of WT and KO mouse aorta. The h-CaD-deficient aorta appeared to have thinner wall and larger diameter, although the number of cell layers in the media section was the same. For the immunofluorescence images the samples were stained with Alexa Fluor 532 phalloidin (200:1 dilution with PBS; for actin) and Hoechst 33258 (1000:1 dilution; for nuclei) according to Eddinger [13]. Scale bars, 0.2 mm for H&E staining and 0.1 mm for the immunofluorescent images.

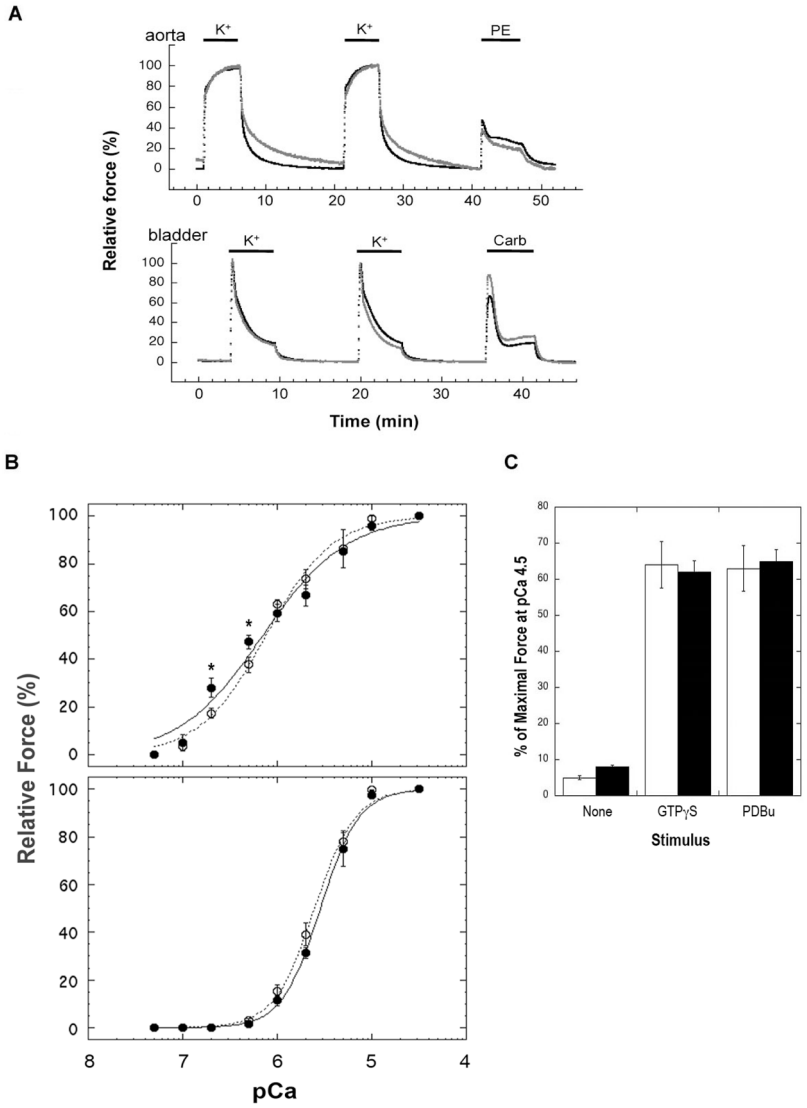

Fig. 4.

A. High K^+ (first two peaks) and phenylephrine- or carbachol-induced (third peak) contractions of intact aorta (upper panel) and urinary bladder (lower panel) from adult WT (black trace) and CaD-KO mice (gray trace). Note that for high K^+-induced contractions of aorta, but not bladder, the relaxation rate of the KO sample is slower than the WT ($p < 0.05$). **B.** Contractile Ca^{2+} sensitivity of α-toxin-permeabilized aorta (upper panel) and bladder (lower panel) in WT (open circles, dot lines) and CaD-KO (closed circles, solid lines) adult mice. Asterisks denote data points with $p < 0.05$. The smooth curves are best fits to the Hill equation (see text). **C.** Relative force generated by GTPγS (30 μM) and PDBu (1 μM) at pCa 6.3 in α-toxin-permeabilized WT (open bars) and KO (closed bars) mouse urinary bladder. All measurements were carried out at 30 °C.

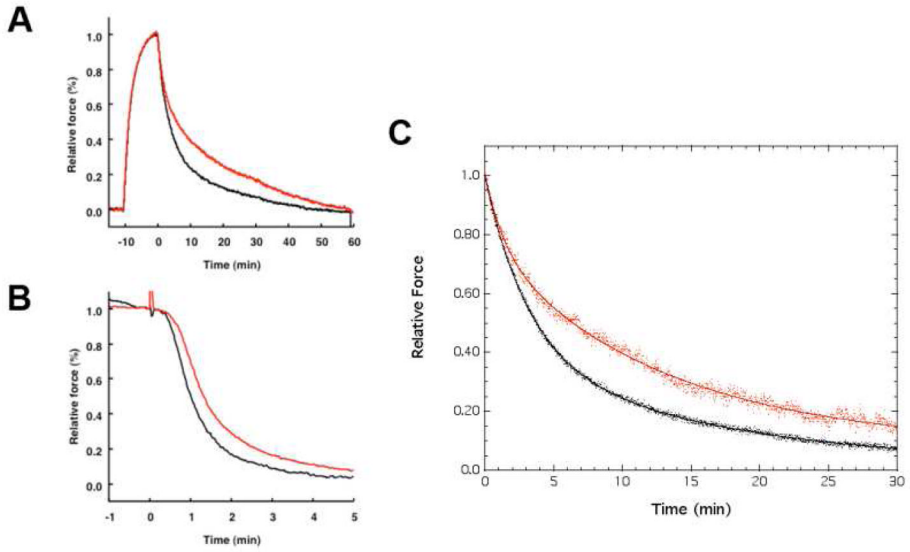

Fig. 5.

A. Time courses of contraction and relaxation of β-escin-permeabilized aorta isolated from WT (black) and h-CaD-KO (red) mice. After permeabilization with β-escin, smooth muscle strips were treated with 10 μM A-23187 for 20 min to deplete Ca^{2+} from the sarcoplasmic reticulum in relaxing solution containing 1 mM EGTA. The strips were stimulated at 20 °C with the pCa 4.5 solution buffered with 10 mM EGTA and relaxed with the Ca^{2+}-free relaxing solution containing 10 mM EGTA (with no added Ca^{2+}) and 300 μM ML-9. **B.** Time courses of relaxation of β-escin-permeabilized tail arteries isolated from WT (black) and h-CaD-KO (red) mice. **C.** Force decay traces of WT (black) and KO (red) aortic tissues (as described in A) were fitted with a bi-exponential equation, which yielded the amplitudes and rate constants.

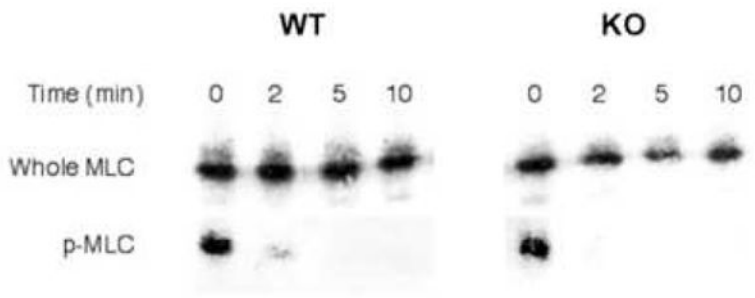

Fig. 6.

Measurements of MLC phosphorylation. α-toxin-permeabilized aortic muscle strips from KO and WT mice were snap frozen at t = 0, 2, 5, and 10 min after onset of relaxation and subjected to quantification of both MLC and phosphorylated MLC by immunoblot analysis. Shown here is a representative result of 3 independent measurements.

Table 1

Summary of relative expression level of CaD in mouse tissues [a]

Tissue	l-CaD^{KO}/l-CaD^{WT}	h-CaD^{WT}	l-CaD^{WT}
Diaphragm	0.33 ± 0.14 (4)	N.D.	0.97 ± 0.48 (4)
Brain	0.37 ± 0.11 (4)	N.D.	0.19 ± 0.04 (4)
Lung	0.44 ± 0.20 (4)	N.D.	0.55 ± 0.24 (4)
Kidney	0.66 ± 0.19 (4)	N.D.	0.31 ± 0.05 (4)
Heart (l.v.)	0.71 ± 0.09 (4)	N.D.	2.84 ± 1.13 (4)
Aorta	0.98 ± 0.06 (5)	0.27 ± 0.08 (3)	0.17 ± 0.04 (5)
Tail Artery	1.03 ± 0.33 (3)	0.06 ± 0.02 (3)	0.04 ± 0.02 (3)
Stomach	1.72 ± 0.23 (4)	N.D.	0.91 ± 0.01 (4)
Intestine	2.67 ± 0.88 (3)	N.D.	0.61 ± 0.12 (3)
Bladder	2.91 ± 0.84 (4)	1.60 ± 0.66 (3)	0.27 ± 0.06 (4)

[a] Results (average ± S.E. with n in parentheses) were based on the digitized immunoblot band intensity of l-CaD normalized to that of β-actin.

Table 2

Summary of fitted parameters of relaxation kinetics[a]

Tissue sample	k_1 (min^{-1})	A_1 (%)	k_2 (min^{-1})	A_2 (%)	n
Aorta					
WT	0.46 ± 0.08	66 ± 5	0.060 ± 0.007	34 ± 5	6
KO	0.71 ± 0.04	32 ± 3	0.081 ± 0.008	68 ± 3	6
Tail artery					
WT	1.71 ± 0.15	81 ± 5	0.40 ± 0.09	19 ± 5	6
KO	1.55 ± 0.26	62 ± 2	0.34 ± 0.07	38 ± 2	6

[a]Average ± SE of 2-component analysis of independent force measurements using β-escin-permeabilized arterial strips taken from age-matched male WT and KO mice.

Pflugers Arch. Author manuscript; available in PMC 2014 February 01.